

Elasticity does not necessarily break down in nanoscale contacts

Comparing stresses from atomistic simulations to continuum theory

Martin H. Müser

Received: date / Accepted: date

Abstract Atomistic structures can have (sharp) features that are not accounted for in standard continuum theories. A prominent example is a Hertzian contact in which, however, the indenting tip is cut out of a crystal, whereby the tip acquires a discretized height profile. The microscopic stresses observed for such quantized indenters show sharp stress peaks at the edges of the height steps so that the stress profiles differ from those produced by smooth, parabolic indenters. Such deviations are frequently misinterpreted as the breakdown of continuum theory at the nanoscale. In this Letter, the stress peaks are confirmed to also occur in a continuum treatment containing steps. In addition, it is shown that analytical solutions for smooth tips can compare extremely well to those with steps if both stress fields are passed through the same (Gaussian) filter smearing out the features in real space with a resolution close to the broadest terrace of the quantized tip. Related statements are shown to also hold for the stress distribution function of randomly rough indenters with quantized height profiles.

1 Introduction

In their well-received papers *The breakdown of continuum models for mechanical contacts* [1] and *Contact of single asperities with varying adhesion: Comparing continuum mechanics to atomistic simulations* [2], Luan and Robbins found – as one of many other results – that contact stresses of indenters with a quantized height

can deviate substantially from the Hertzian continuum-mechanics based solution. Although Luan and Robbins correctly state in the title of their paper that the *models* break down, these deviations are often interpreted by others as a sign for the automatic breakdown of continuum mechanics at the nanoscale altogether. This cannot be correct in the context of a phenomenon such as linear or close-to-linear elasticity, which is essentially scale free down to atomic dimensions.

In fact, Luan and Robbins find the load-displacement curve to be much less affected by the steps than the normal stress profiles. Significant deviations only occur at small loads when few terraces of the stepped indenter are in contact [1,2]. In this limit results can also be affected by the finite range of surface interactions and atomic discreteness, which could also be included in more accurate continuum theories. Moreover, Luan and Robbins already emphasize themselves that *continuum mechanics could be applied to smaller contacts if the true atomic-scale surface roughness was included*.

This claim was later confirmed through large-scale simulations by Medina and Dini [3], who demonstrated that the sharp features of stresses occurring due to stepped indenters also appear in continuum treatments. Yet, the misinterpretation of the automatic breakdown of substrate elasticity at the nanoscale persists. Certainly, when external forces or adhesion are sufficiently large to lead to a strongly non-linear response including plastic deformation, continuum mechanics can break down at the nanoscale. However, Luan and Robbins imposed deformations, which were sufficiently small for them to state: *We present results for ideal harmonic crystals, but find similar results for Lennard-Jones interactions*.

The author of this paper feels that another, detailed analysis of the stepped Hertzian contacts facilitates the

M. H. Müser
Department of Materials Science and Engineering, Saarland University, Campus C6 3, 66123 Saarbrücken, Germany E-mail: martin.mueser@mx.uni-saarland.de

correct interpretation of Luan and Robbins' work. Towards this end, continuum-mechanics simulations are conducted, whose results – like Medina and Dini's results [3] – bear much similarity with the mentioned atomistic simulations. At the same time, it is explored to what extent the continuum solution for smooth tips compares to the solution for stepped tips, if both stress fields are coarse grained with a similar filter reducing the in-plane spatial resolution of the data. This procedure of comparing atomistic to coarse-grained simulations may allow a resolution-dependent contact area to be defined in atomistic simulations, even when repulsive forces have a finite rather than a zero range.

Since the effect of quantized indenter heights on stresses is an interesting topic, this work also investigates how discrete heights alter the local microscopic stresses and their distribution function in contacts of randomly rough surfaces. Discrete steps correspond to correlated roughness, which are not accounted for in contact-mechanics theories assuming the random-phase approximation for the height Fourier coefficients [4]. It is therefore also explored to what extent the proposed stress coarsening procedure benefits the analysis of large-scale contacts.

The numerical method of this work is Green's function molecular dynamics (GFMD) [5] in a new variant combining two optimization schemes [6]. While it may be worth mentioning that the Hertz problem defined in Sect. 2.1 can be solved in 10 s on a standard desktop computer with the new GFMD code, the author abstains from its presentation in this short communication, because the method is well established [7] and the new variant described in detail elsewhere [6]. The remainder of this Letter therefore only contains a results and a conclusions section.

2 Results

2.1 Hertzian indenters

We first examine the effect of the shape of a rigid, frictionless indenter on the purely continuum response in an ideal elastic substrate. A smooth indenter is compared to a tip with steps that might represent the atomic terraces on a nanometer tip as investigated in Refs. [1, 2], but could equally well be microns high. **In principle, the given** ~~The such defined~~ problem has no intrinsic scale and the discretization used in the numerical solution is not connected to **real** atoms **even if a discretization point may be called a superatom – whereby the subtitle of this article can be justified.** As discussed in Refs. [1,2], **real** atomic discreteness may introduce

many additional effects, which, however, are not the focus here.

More specifically, we consider a Hertzian contact geometry consisting of a stiff, frictionless parabolic indenter with a radius of curvature R , which is squeezed against a flat, linearly elastic solid having a contact modulus E^* . The (default) load is set to $L = 0.01 E^* R^2$. The analytical solution to this problem is well known and summarized in text books on contact mechanics [8]. For example, the contact radius is $a_c = \sqrt[3]{3LR/4E^*}$ and the peak pressure is $p_0 \approx \sqrt[3]{6FE^{*2}/R^2/\pi}$, which in our case leads to $a_c \approx 0.1957 R$ and $p_0 = 0.1246 E^*$ for the smooth parabolic indenter. Relative deviations of the numerical data — $a_c(\text{GFMD}) \approx 0.1947 R$ (sub-grid resolution can be obtained from fits to the stress near the contact edge) and $p_0(\text{GFMD}) \approx 0.1258 E^*$ — to the analytical Hertz solution are less than 1%. They arise from two effects: (i) Periodic boundary conditions are employed within the plane with a simulation-box length of $\mathcal{L} = R$. (ii) Real space is discretized into elements having a linear dimension of $R/512$ rather than into infinitesimally small elements. Note that because we are in the linear, scale-free limit, the results for these two geometries can be mapped to a continuum of isomorphic problems. For example, doubling R and halving L would leave the contact radius unchanged but reduce the pressures and strains by a factor of $2^{2/3}$.

Besides the smooth indenter, we also consider a tip with discrete heights separated by integer multiples of $\Delta h = R/200$. An outer step-wise approximation to the parabolic shape was chosen, because it leads to the largest possible flat terrace and thereby to a maximum discrepancy between the stress profile of the smooth and a step-wise constant profile. The geometry of the tips is shown in Fig. 1.

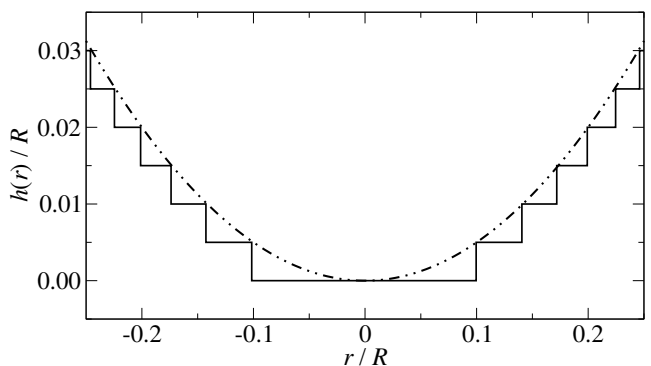


Fig. 1 Height profile of a continuous (broken lines) and a stepped (solid lines) Hertzian tip. The step height is $R/200$. Note that the abscissa and the ordinate are normalized in the same way but they are not to scale.

Hard-wall interactions are used to describe the interactions between the surfaces. There are three main reasons for this choice: First, and most importantly, if body rather than surface forces are used in the atomistic simulations, then the continuum treatment should also be based on body forces and not describe a different system. Second, the use of hard-wall interactions allows contact area to be defined unambiguously. Third, realistic characteristic lengths ρ for exponential repulsion (not adhesion, which may be much longer ranged) are typically a quarter of an interatomic spacing a , i.e., a is in the order of a bohr. Fig. 11 of Ref. [5] reveals that when ρ is small compared to the characteristic lengths defining the contact, the effect of finite-range repulsion is predominantly a smearing out of the stress kink at the contact edge. This smearing out is less substantial and less broad than the effect that the height plateaus have on the stress profile, except at very small loads.

The stress profiles differ radically between stepped and non-stepped indenters at the investigated load, as can be seen in the top panel of Fig. 2. The quantized indenter leads to the previously observed [1,3] stress peaks at the edge of each step, while the continuous indenter shows the well-known continuous stress profile. Yet both solutions appear to resemble each other and the question arises if a well-defined coarse graining reveals that similarity.

One possibility to check for resemblance between both data sets is to apply a similar local averaging, or filter, to both stress profiles. For this study, a Gaussian filter was explored. The reason for this choice was predominantly that a Gaussian folded with a second Gaussian remains Gaussian. In addition, a Gaussian decays asymptotically more quickly than an exponential so that a Gaussian could be said to lead to a more local smearing than an exponential filter. The Gaussian filter coarse-grains the stress profile according to

$$\sigma_{\text{cg}}(\mathbf{r}) = \frac{1}{2\pi\Delta r^2} \int d^2r' e^{-(\mathbf{r}-\mathbf{r}')^2/2\Delta r^2} \sigma(\mathbf{r}'), \quad (1)$$

where Δr is a measure of the length scale over which the stress is locally averaged. The filter is rather easily implemented in a Fourier-based Green's function code like ours. It basically requires only one additional line of code, e.g., in our code,

```
stress[iQ] *= exp(-(dr*q[iQ])^2/2).
```

This command must be invoked before the inverse Fourier transform is taken, because the Fourier representation of Eq. (1) reads

$$\tilde{\sigma}_{\text{cg}}(\mathbf{q}) = e^{-\Delta r^2 q^2/2} \cdot \tilde{\sigma}(\mathbf{q}). \quad (2)$$

The result of such a coarse-graining procedure is shown in Fig. 2. Note that the stress peaks at the edges

of the steps in the fully resolved calculation would turn into stress singularities in the limit of infinitesimally small discretization. Finer discretizations than those presented here are easily possible, but do not noticeably change the shown coarse-grained stress profiles, except that the stress singularities result in higher peaks. Very large peaks, however, would ultimately induce a plastic response in a real system, as discussed, for example in Ref. [10].

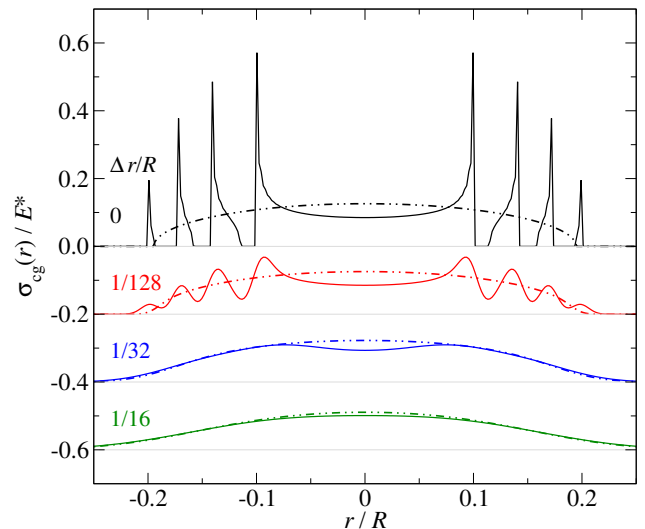


Fig. 2 Coarse-grained stress $\sigma_{\text{cg}}(r)$ of the investigated continuous (broken lines) and the quantized (solid lines) Hertzian tip as a function of the distance r from the symmetry axis. In the top panel, no filter was applied. In the remaining panels, filters smearing out the stress with different resolutions Δr are employed. Successive curves are shifted downward to avoid mutual overlap. Thin gray lines indicate the respective reference abscissa.

Fig. 2 reveals that coarse-graining makes the original and the stepped solution approach each other quite closely even when the broadening width Δr is clearly less than the width of the broadest terrace w_t , which takes the value of $w_t = 0.1 R$ in the current case study. For $\Delta r \approx w_t/2$, the coarse-grained continuum and the stepped solution are already almost indistinguishable, as can be seen for the $\Delta r = R/16$ curve in Fig. 2.

An effective coarse graining of stresses also occurs naturally as a function of depth, as expressed by Saint-Venant's principle. It states that the details of the stress distribution on a scale a barely matter at a depth $3a$ [1]. Recent simulations by Klemenz *et al.* [11] revealed an impressive example for Saint-Venant's principle: a single graphene layer deposited on top of a stepped metal regularizes quite noticeably its mechanical response. For our problem of interest, the question thus arises how the stress profiles of smooth and stepped indenters dif-

fer in the bulk as a function of depth. A particular depth is $d = 0.78 a_c$, where the continuum profile has the largest shear stress. Fig. 3 reveals that the normal stresses at this depth produced by the smooth and the considered stepped profiles show maximum deviations of order 10%. The observed differences at that critical depth are therefore noticeable but yet much reduced compared to those of the surface stresses. Similar statements hold for other stress-tensor elements including the von Mises stress, which were computed as described recently [9]. However, the numerical values for von Mises stress also depend on the Poisson ratio.

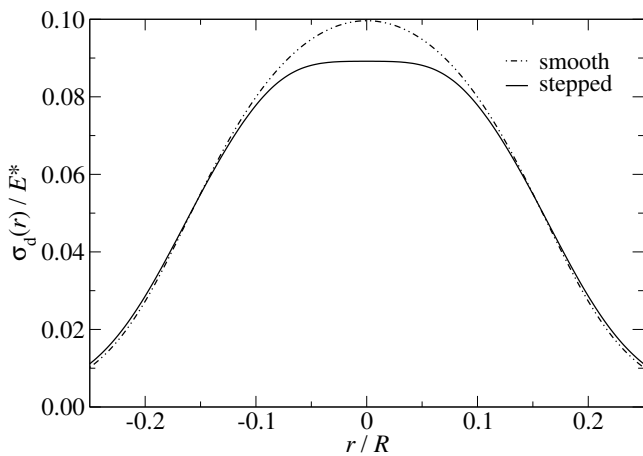


Fig. 3 Stress profile of the smooth and stepped indenter at the depth $d = 0.78 a_c$, where the smooth tip has the largest shear stress.

Note that the coarsening of stress with depth differs from that considered here. Different wave vectors coarsen essentially exponentially with depth z , e.g., with $\exp(-qz)$ or with $(1 + qz) \exp(-qz)$. In the Gaussian coarsening procedure proposed here, the Fourier components are instead multiplied with $\exp(-\Delta r^2 q^2/2)$.

We conclude this section with a discussion of the question how many steps need to be in contact in order for the stress coarsening procedure to be effective. However surprising it may sound, contact with one single step is sufficient. If the filtering is done with Δr being half a terrace width, the filtered original Gaussian and the filtered stepped stress profiles look already quite similar. A maximum relative difference in the stress of a little less than 20% occurs. Increasing Δr to the full width of the terrace reduces that error to 4%.

For completeness, we also comment on the normal displacement d , even if the $d(L)$ relation is unrelated to the stress-coarsening procedure proposed in this work. While making contact solely with a single step, d is linear in L , as for the flat punch solution. This relation

obviously differs from the $d \propto L^{2/3}$ proportionality of the original Hertzian-contact geometry. For the $d(L)$ relation of stepped and unstepped indenters to resemble each other, several steps need to be in contact. This is in line with the observations of Luan and Robbins [1, 2], who found the biggest deviations from Hertz in the limit of small numbers of contacting steps.

2.2 Stepped, randomly rough indenters

The presence of stress singularities at the edges of steps brings up the interesting question how height quantization affects the stress in contacts of elastic solids in contact with randomly rough indenters. To address this question, the contact mechanics of such surfaces is computed using GFMD and compared to their continuous counterparts. This includes a comparison of the stresses in real space as well as of their distribution function $\text{Pr}(\sigma)$.

A model for randomly rough surfaces is used which is similar to those that have been routinely simulated for a little more than a decade [7, 12–16]. It is based on a surface height spectrum $C(q) \equiv \langle |\tilde{h}^2(\mathbf{q})| \rangle$ having the functional form [17–19]

$$C(q) = \frac{C_0 \Theta(q_s - q)}{\{1 + (q/q_r)^2\}^{1+H/2}}. \quad (3)$$

Here $\tilde{h}(\mathbf{q})$ is the complex Fourier transform of the height profile. Its absolute value is set to $\sqrt{C(q)}$ and its phase is assigned a uniform random variable on $(0, 2\pi)$. Moreover, $q_r = 2\pi/\lambda_r$ and $q_s = 2\pi/\lambda_s$ represent the roll-off wavevector and high-wavevector cutoff, respectively, while $\Theta(\dots)$ is the Heavyside step function. The prefactor C_0 is chosen such that the root-mean square (rms) height gradient \bar{g} equals unity, but the results are isomorphic to solutions for arbitrary slope in the linear, scale-free limit considered here. The calculations presented in this work are based on the following parameters $\mathcal{L}/\lambda_r = 3$, $\lambda_r/\lambda_s = 100$, and λ_s/a varying from 3.4 to 27.3. H is called the Hurst roughness exponent, which is set to its generic value of $H = 0.8$.

Stepped height profiles are realized by replacing the initially drawn height $h(\mathbf{r})$ with $\Delta h \cdot \text{int}\{h(\mathbf{r})/\Delta h\}$. For the case study presented here, $\Delta h = \lambda_r/200$ was chosen. The studied height profiles along a cut at $x = \mathcal{L}/2$ are shown in Fig. 4.

The interaction between the indenter and the flat, linear elastic body is a hard-wall repulsion as for the Hertzian indenter. The two bodies are squeezed against each other with a normal pressure of $p_0 = 0.01E^*\bar{g}$, which leads to a relative contact area of $a_r \approx 0.02$. Fig. 5 shows the resulting stress for both continuous

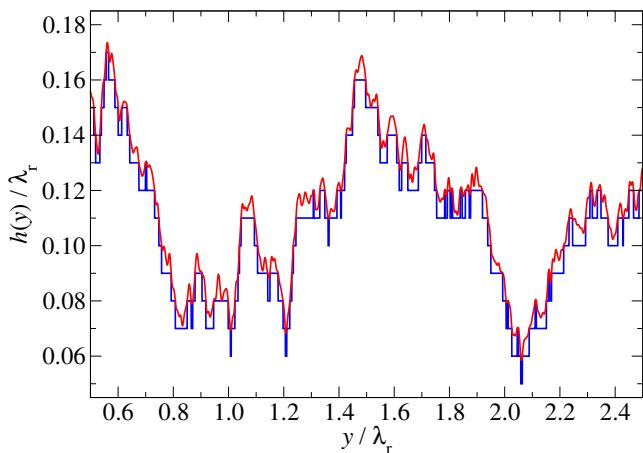


Fig. 4 Surface topography of the original smooth (red line) and the stepped (blue line) height profile along a cut at $x = L/2$ through the surface.

and stepped stress height profiles. Without much spatial resolution, the distribution of contact stresses appear quite similar in both cases, even if there is no one-to-one match regarding each individual contact patch.

When contemplating the stresses locally, clear differences between the stress produced by continuous and stepped indenters can be appreciated. These differences, however, disappear when the data at the small scale (e.g., at the atomic scale) is processed through a Gaussian filter of the same form as in Eq. (1). In a boundary-element code, $\sigma(\mathbf{r})$ is known on a suitable grid and likewise the stress is known in Fourier space, in which case the coarsening can be readily done in the Fourier representation via Eq. (2). After applying the filter to both stress fields, i.e., the one resulting from the smooth and the one from the stepped random roughness, the two stress distributions look rather similar.

In passing we note that a similar smoothing procedure can also be applied to conventional atomistic simulations, which are not boundary-element method based like GFMD. An atom i below a plane with a surface normal to the z -axis can be assigned a surface stress of the form $\sigma_{3\alpha}(\mathbf{r}) = F_{n\alpha}\delta(\mathbf{r}-\mathbf{r}_n)$, where $\delta(\dots)$ is the Dirac delta function, \mathbf{r}_n the in-plane coordinate of the atom, and $F_{n\alpha}$ the force acting on atom n , which is due to the presence of atoms on the other side of the plane. [20] For truly atomic simulations it might therefore be best to use Eq. (1), or, when the coarsening length Δr is large, to assign the forces in an appropriate fashion to bins.

We come back to the issue of stresses in randomly rough surfaces. Often, it is not useful to know the stress in a spatially resolved manner, but the microscopic distribution function $\text{Pr}(\sigma)$ may be of interest. $\text{Pr}(\sigma)\Delta\sigma$

states the probability that a randomly picked surface point in the interface is assigned a stress within $\sigma \pm \Delta\sigma/2$ in the limit $\Delta\sigma \rightarrow 0$. Fig. 6 reveals that the functional form of the microscopic stress distribution functions differ between the two cases. In particular, if the total probability density is written as

$$\text{Pr}(\sigma)\Delta\sigma = (1 - a_r)\delta(\sigma) + a_r \cdot \text{Pr}_c(\sigma)\Delta\sigma, \quad (4)$$

it is found that a frequently used, analytical approximation to $\text{Pr}_c(\sigma)$ [4] satisfying

$$\text{Pr}_c(\sigma) \propto e^{-(\sigma-p_0)^2/2\Delta\sigma^2} - e^{-(\sigma+p_0)^2/2\Delta\sigma^2}, \quad (5)$$

with $\Delta\sigma^2 = (E^*\bar{g}/2)^2$, describes the stresses very well for $\sigma > E^*\bar{g}$ in the case of smooth surfaces. In contrast,

$$\text{Pr}_c(\sigma) \propto \frac{1}{1 + (\sigma/\sigma_{\text{ref}})^{2.4}} \quad (6)$$

approximates the contact-stress distribution quite well for stepped surfaces for all σ .

As a side comment, it is noted that Eq. (5) was reported earlier to be inaccurate for the stress distribution function for $\sigma < E^*\bar{g}$ for regular, randomly rough surfaces and that $\text{Pr}(\sigma \rightarrow 0)$ obeys a power law, in which $\text{Pr}(\sigma)$ grows approximately as $\sigma^{0.7}$ at small σ [21], which is consistent with the data produced for this study.

While the functional forms of the stress distribution differ for smooth and stepped, randomly rough surfaces, their first moments turn out quite similar. In both models, the dimensionless ratio $\kappa \equiv a_c E^*\bar{g}/p_0$ turns out $\kappa = 2$ within 1%, confirming previous results on stepped, elastic indenters [10]. This means that the first moment of the stress averaged only over the contact is $\langle\sigma\rangle_{\text{contact}} \approx E^*\bar{g}/2$ for the smooth and the considered stepped profile, where, however, \bar{g} denotes the rms-gradient of the *original* surface.

Finally, Fig. 7 addresses the question if the stress distribution functions of smooth and stepped randomly rough surfaces become similar to each other when a Gaussian broadening is applied to both of them. Due to the Gaussian filter, the non-contact δ -function contribution leads to significant contributions at small values of σ , which were not present before. At the same time, the broad tails of the stress distribution for stepped surfaces has disappeared and turned into a similar asymptotic behavior as for the continuous surfaces. In fact, at the given moderate amount of smoothing, the tails at large stresses still resembles the analytical solution of Eq. (5).

It appears that smearing out the stress fields with a resolution $\Delta r \lesssim \lambda_s$ suffices to invoke a relatively close resemblance between the σ_{cg} distributions for stepped

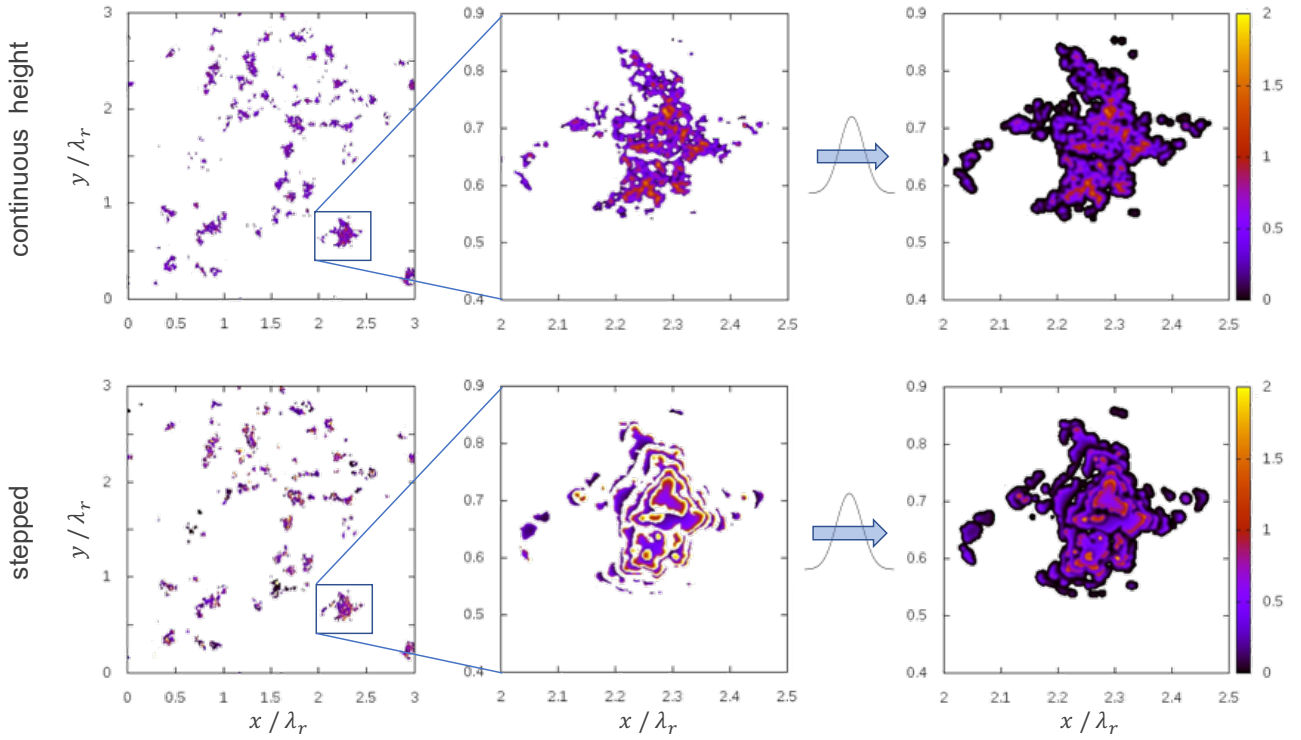


Fig. 5 Stress in contacts between a randomly rough, rigid indenter and a flat, linearly elastic solid. Top and bottom rows refer to continuum and stepped heights, respectively. The left column shows the stress on the entire simulation cell. The middle column shows the stress on a selected meso-scale contact patch, while the right column shows the same stress after having been coarse-grained through a Gaussian filter with a resolution of $\Delta r = 0.006 \lambda_r$.

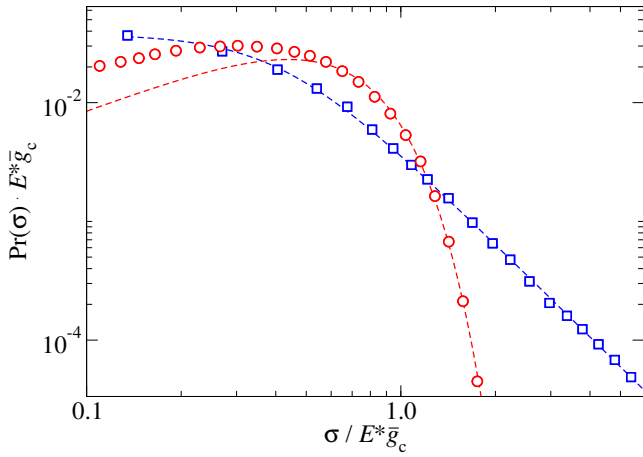


Fig. 6 Stress distribution function of the original (red circles) and the stepped (blue squares) randomly rough surface. The dashed red and blue line represent, Eq. (5) and Eq.(6), respectively.

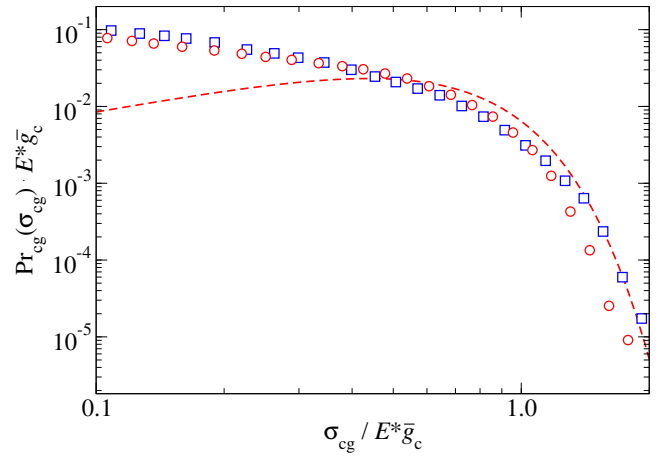


Fig. 7 Stress distributions of the local stress resulting from the microscopic stress distribution after coarse-graining using Eq. (1) with $\Delta r = 0.6 \lambda_s$. All stresses are normalized with the rms-gradient of the continuous surface \bar{g}_c .

and smooth, random surfaces. However, the same statement does not quite hold for the real-space data. Remnants of stress singularities at the edge of “large” terraces, whose linear size clearly exceeds $\lambda_s = 0.01 \lambda_r$, are still noticeable in the lower right panel of Fig. 5.

A brief discussion might be in place regarding the asymptotic $\sigma \rightarrow 0$ behavior of the stress distribution function. As in early numerical studies of randomly rough contacts [12], the coarse-grained $\text{Pr}(\sigma)$ increases towards small σ , in contradiction to the prediction by

Persson theory of a linear relationship [4] or the sublinear power law identified in high-resolution GFMD simulations [21]. The reason for this discrepancy is that the coarse-graining also effects the displacements so that they implicitly have a high-wavenumber cutoff at a similar scale where roughness is smoothed or cut off. In contrast, continuum theory and the high-resolution GFMD simulation assume elastic response functions at wavevectors that exceed the high-wavenumber cutoff of the surface roughness.

3 Conclusions

Robbins and Luan [1, 2] provided the useful insight that classic Hertz and related adhesive models are not accurate in contacts that approach atomic dimensions, as common for atomic force or other scanning probe microscopy. New length scales and phenomena become important at these scales that are not included in the classic theories. One is the presence of height fluctuations that lead to strong oscillations in the surface stress. As they noted, these are related to changes in geometry that are not included in Hertz theory. Unfortunately these oscillations have often been interpreted by others as a sign of a universal failure of elasticity at small scales.

In this paper, we have confirmed that these stress oscillations do not reflect a failure of elasticity but rather the elastic response to the true surface geometry [1–3]. Moreover, we demonstrate that the analytical solution for a Hertzian indenter compares extremely well to the numerical solution for a stepped Hertzian surface, when the stress fields of both calculations are passed through the same (Gaussian) filter with a resolution slightly more than half the maximum terrace. Although the continuum flat punch solution would certainly be the appropriate model in the limit of a single plateau, the coarsened original and the coarsened stepped Hertzian profile still resemble each other in this extreme limit.

The presented simulations also revealed that stepped, randomly rough surfaces can be described in terms of recent contact mechanics theories taking the height spectra as input, i.e., Persson’s contact mechanics theory [4]. However, such theories are only valid up to the inverse wavelengths, at which the steps lead to significant tails in the surface spectrum. When including wave vector components of the spectra, which arise due to the steps and for which correlation matters, Persson theory (in its present form) is not yet in a position to make correct predictions for the stress distribution functions. The theory always predicts Gaussian tails for $\text{Pr}(\sigma)$, while the distribution function is clearly algebraic for stepped

surfaces. It had been speculated earlier that possible deviations of the random-phase approximation present in real surfaces induces non-Gaussian – more slowly decaying – asymptotics of $\text{Pr}(\sigma)$ at large stresses [13]. Thus, addressing correlation in randomly rough contacts remains a theoretical challenge to be solved.

The comparison between a continuum model and an atomistic model is only fair when the continuum model is an accurate representation of the full model. Otherwise, either the model has to be refined or, as demonstrated in this work, the results from the full and the continuum model have to be passed through an appropriate filter reducing the spatial resolution. Thus, when atomistic simulations do not appear to match up with continuum simulations, it may well be that the comparison is not ideal rather than that continuum theory is invalid. This last line is not intended to criticize the papers by Luan and Robbins [1, 2], since they stated that their simulations were affected by the directionality, finite range, and finite stiffness of interfacial interactions as well as by atomic discreteness. Nonlinear response, plasticity, and other phenomena may also be important in contacts with atomic dimensions. These effects are not in traditional continuum models used in the tribology community, but could be included.

To conclude the paper (though the following text could have also been placed into the Introduction), it might be worth reflecting the meaning of the sentence *Continuum mechanics breaks down*. Two questions need to be addressed: Where does continuum mechanics end and when does it break down? In the author’s opinion, continuum mechanics knows body forces, strain fields may have an upper wavenumber limit (which would be commonly set to π over the atomic spacing), and continuum corrections can be applied, e.g., in the form of realistic dispersion relations for bulk phonons or stress-displacement relations of semi-infinite bodies. None of these features are reflected for good reasons in the Hertz model. A beyond-the-norm sophisticated attack of continuum mechanics on a specific contact problem, however, would incorporate them. If large discrepancies between such a treatment and full atomistic simulations persisted, only then should continuum mechanics be said to have broken down. An extremely sophisticated continuum-mechanics approach might even include the atomic-scale undulations of the substrate potential, as done in approaches to the Frenkel-Kontorova model [22] and thereby rationalize or even quantify the effect of crystalline alignment on interfacial shear forces, which are commonly treated as ugly add-ons in continuum mechanics.

Acknowledgments MM thanks Mark O. Robbins for extensive and helpful feedback on the manuscript.

References

1. Binquan Luan and Mark O. Robbins. The breakdown of continuum models for mechanical contacts. *Nature*, 435(7044):929–932, jun 2005.
2. Binquan Luan and Mark O. Robbins. Contact of single asperities with varying adhesion: Comparing continuum mechanics to atomistic simulations. *Physical Review E*, 74(2):026111, aug 2006.
3. Simon Medina and Daniele Dini. A numerical model for the deterministic analysis of adhesive rough contacts down to the nano-scale. *International Journal of Solids and Structures*, 51(14):2620–2632, jul 2014.
4. B. N. J. Persson. Theory of rubber friction and contact mechanics. *The Journal of Chemical Physics*, 115(8):3840, 2001.
5. Carlos Campañá and Martin H. Müser. Practical Green’s function approach to the simulation of elastic semi-infinite solids. *Phys. Rev. B*, 74(7):075420, aug 2006.
6. Y. Zhou, M. Moseler, and M. H. Müser. Solution of boundary-element problems using the fast-inertial-relaxation-engine method. (submitted).
7. M. H. Müser, W. B. Dapp, R. Bugnicourt, P. Sainsot, N. Lesaffre, T. A. Lubrecht, B. N. J. Persson, K. Harris, A. Bennett, K. Schulze, S. Rohde, P. Ifju, W. G. Sawyer, T. Angelini, H. Ashtari Esfahani, M. Kadkhodaei, S. Akbarzadeh, J.-J. Wu, G. Vorlauffer, A. Vernes, S. Solhjoo, A. I. Vakis, R. L. Jackson, Y. Xu, J. Streater, A. Rostami, D. Dini, S. Medina, G. Carbone, F. Bottiglione, L. Afferrante, J. Monti, L. Pastewka, M. O. Robbins, and J. A. Greenwood. Meeting the contact-mechanics challenge. *Tribology Letters*, 65(4), aug 2017.
8. K. L. Johnson. *Contact mechanics*. Cambridge University Press, Cambridge, UK, 1985.
9. Martin H. Müser. Internal, elastic stresses below randomly rough contacts. *Journal of the Mechanics and Physics of Solids*, 119:73–82, oct 2018.
10. Lars Pastewka, Tristan A. Sharp, and Mark O. Robbins. Seamless elastic boundaries for atomistic calculations. *Physical Review B*, 86(7):075459, aug 2012.
11. Andreas Klemenz, Adrien Gola, Michael Moseler, and Lars Pastewka. Contact mechanics of graphene-covered metal surfaces. *Applied Physics Letters*, 112(6):061601, feb 2018.
12. S. Hyun, L. Pei, J.-F. Molinari, and M. O. Robbins. Finite-element analysis of contact between elastic self-affine surfaces. *Physical Review E*, 70(2):026117, aug 2004.
13. C. Campañá and M. H. Müser. Contact mechanics of real vs. randomly rough surfaces: A Green’s function molecular dynamics study. *Europhysics Letters (EPL)*, 77(3):38005, jan 2007.
14. C. Putignano, L. Afferrante, G. Carbone, and G. Deme-lio. The influence of the statistical properties of self-affine surfaces in elastic contacts: A numerical investigation. *Journal of the Mechanics and Physics of Solids*, 60(5):973–982, may 2012.
15. N. Prodanov, W. B. Dapp, and M. H. Müser. On the contact area and mean gap of rough, elastic contacts: Dimensional analysis, numerical corrections, and reference data. *Tribology Letters*, 53(2):433–448, dec 2014.
16. V. A. Yastrebov, G. Anciaux, and J.-F. Molinari. From infinitesimal to full contact between rough surfaces: Evolution of the contact area. *International Journal of Solids and Structures*, 52:83–102, jan 2015.
17. A. Majumdar and C. L. Tien. Fractal characterization and simulation of rough surfaces. *Wear*, 136(2):313–327, mar 1990.
18. G. Palasantzas. Roughness spectrum and surface width of self-affine fractal surfaces via the k-correlation model. *Physical Review B*, 48(19):14472–14478, nov 1993.
19. B. N. J. Persson. On the fractal dimension of rough surfaces. *Tribology Letters*, 54(1):99–106, mar 2014.
20. B. D. Todd, Denis J. Evans, and Peter J. Daivis. Pressure tensor for inhomogeneous fluids. *Physical Review E*, 52(2):1627–1638, aug 1995.
21. A. Wang and M. H. Müser. Gauging Persson theory on adhesion. *Tribol. Lett.*, 65(3):103, jun 2017.
22. Oleg M. Braun and Yuri S. Kivshar. Nonlinear dynamics of the frenkel-kontorova model. *Physics Reports*, 306(1-2):1–108, dec 1998.